Explicit definition of $\mathcal{PT}$ symmetry for nonunitary quantum walks with gain and loss

Ken Mochizuki, Dakyeong Kim, and Hideaki Obuse
Department of Applied Physics, Hokkaido University, Sapporo 060-8628, Japan
(Received 30 March 2016; published 17 June 2016)

$\mathcal{PT}$ symmetry, that is, a combined parity and time-reversal symmetry, is a key milestone for non-Hermitian systems exhibiting entirely real eigenenergy. In the present work, motivated by a recent experiment, we study $\mathcal{PT}$ symmetry of the time-evolution operator of nonunitary quantum walks. We present the explicit definition of $\mathcal{PT}$ symmetry by employing a concept of symmetry time frames. We provide a necessary and sufficient condition so that the time-evolution operator of the nonunitary quantum walk retains $\mathcal{PT}$ symmetry even when parameters of the model depend on position. It is also shown that there exist extra symmetries embedded in the time-evolution operator. Applying these results, we clarify that the nonunitary quantum walk in the experiment does have $\mathcal{PT}$ symmetry.

DOI: 10.1103/PhysRevA.93.062116

I. INTRODUCTION

Quantum mechanics requires that, in a closed system, physical observables be represented by Hermitian operators. The Hamiltonian of the system is no exception to this rule. However, the closed system is an ideal concept and, rigorously speaking, almost all systems in the real world, except a whole universe, should have flow of energy and particles to outer environments, which makes the Hamiltonian of the inner system non-Hermitian. Furthermore, it is widely accepted to phenomenologically include non-Hermitian effects into Hamiltonians when we treat effects of amplification and dissipation, namely, gain and loss, in open systems. For example, non-Hermitian Hamiltonians are employed to describe radioactive decay [1], depinning of flux lines in type-II superconductors [2], and so on [3]. In general, such a non-Hermitian Hamiltonian has complex eigenenergy which makes systematic controls of the dynamics difficult.

In 1998, however, Bender and Boettcher clarified that a broad class of non-Hermitian Hamiltonians can have entirely real eigenenergy if the system possesses a combined parity symmetry and time-reversal symmetry (TRS), that is, $\mathcal{PT}$ symmetry [4–7]. If the Hamiltonian possesses $\mathcal{PT}$ symmetry and its eigenstates are also eigenstates of the $\mathcal{PT}$-symmetry operator, then this is a sufficient condition for the eigenenergy being real. Applying this property, moreover, $\mathcal{PT}$ symmetry in the non-Hermitian Hamiltonian provides a procedure to selectively induce complex eigenenergy for specific eigenstates [8–10]. For systems described by non-Hermitian Hamiltonians with $\mathcal{PT}$ symmetry, a large number of novel phenomena, which can not be observed in Hermitian systems, have been predicted theoretically. For example, systems with $\mathcal{PT}$-symmetric periodic structures can act as unidirectional invisible media [11,12], edge states having complex eigenenergy emerge [13,14], Bloch oscillations with unique features occur [15], and others [16–24]. These results open a way to engineer non-Hermitian systems to utilize as novel platforms of applications. The system with $\mathcal{PT}$ symmetry has been realized in optics by using coupled optical waveguides with fine-tuned complex refractive index [25,26]. It has been also demonstrated that coupled microcavity resonators realize $\mathcal{PT}$-symmetric systems [27,28]. Recently, the mode-selective lasing by utilizing $\mathcal{PT}$ symmetry has been realized based on microring resonators [29,30]. However, due to difficulty in handling gain and loss effects, the experimental systems are limited to a small number of elements.

In contrast, there is a unique way to experimentally perform large-scale $\mathcal{PT}$-symmetric systems with high tunability, that is, the discrete-time quantum walk [31,32]. The discrete-time quantum walk (quantum walk, in short) is the model recently attracting attention as a versatile platform for quantum computations and quantum simulators. The quantum walk describes quantum dynamics of particles by a time-evolution operator, instead of a Hamiltonian. Quantum walks have been realized in various experimental setups, such as cold atoms [33], trapped ions [34,35], and optical systems [36–40]. Since quantum walks enable high tunability of the system setup, various phenomena which require delicate setups have been observed, such as Anderson localization [41,42], scattering with positive- and negative-mass pulses [43], emergence of edge states which stem from topological phases [44], and so on.

Remarkably, in 2012, a quantum walk by optical-fiber loops, where additional optical amplifiers make it possible to control the effects of gain and loss, was experimentally implemented [45]. Due to gain and loss, the time-evolution operator of this quantum walk becomes nonunitary, which can be considered that the effective Hamiltonian is non-Hermitian. Nevertheless, it has been shown that the system has entirely real (quasi)energy in proper setups. Furthermore, interesting phenomena peculiar to $\mathcal{PT}$ symmetry, such as unidirectional invisible transport [45], extraordinary Bloch oscillations [45], and optical solitons [46,47], have been observed. These results provide convincing evidence that the system possesses $\mathcal{PT}$ symmetry. However, $\mathcal{PT}$ symmetry and the $\mathcal{PT}$-symmetry operator have not yet been directly identified from the time-evolution operator itself, since the definition of $\mathcal{PT}$ symmetry on the time-evolution operator has not been established so far. It is an urgent and important task to identify the explicit definition of $\mathcal{PT}$ symmetry for further developments.

In the present work, we provide the explicit definition of the $\mathcal{PT}$-symmetry operator and identify that the time-evolution operator of the nonunitary quantum walk in the experiment has, indeed, $\mathcal{PT}$ symmetry. This is archived for the first time by employing a concept of symmetry time frames [48] which has been developed in the recent study of topological phases of quantum walks [48–52]. We also show that the time-evolution operator of the nonunitary quantum walk has

extra symmetries. Furthermore, we provide the necessary and sufficient conditions for $\mathcal{PT}$ and other symmetries of the time-evolution operator even when parameters of the model are position dependent. Taking account of these results, we present an inhomogeneous nonunitary quantum walk with $\mathcal{PT}$ symmetry. (We note that, although the argument on $\mathcal{PT}$ symmetry to retain the reality of (quasi)energy has been generalized in Refs. [53–55], we focus on $\mathcal{PT}$ symmetry in the original sense of Ref. [4] in the present work.)

This paper is organized as follows. We define the time-evolution operator of the nonunitary quantum walk in Sec. II. Section III is devoted to presenting how to define and identify $\mathcal{PT}$ symmetry and extra symmetries of the time-evolution operator of the nonunitary quantum walk. This is our main result of the present work. In Sec. IV, as applications of the result obtained in the previous section, we identify $\mathcal{PT}$ symmetry of the time-evolution operator of the nonunitary quantum walk in the experiment [45] and, further, demonstrate a $\mathcal{PT}$-symmetric inhomogeneous nonunitary quantum walk. The summary and discussion are given in Sec. V.

II. DEFINITION OF TIME-EVOLUTION OPERATORS OF NONUNITARY QUANTUM WALKS

Figure 1 shows the schematic view of the experimental setup of the nonunitary quantum walk implemented by the two optical-fiber loops in Ref. [45]. As explained in the caption, the system is interpreted as one-dimensional (1D) two-step quantum walks. Motivated by the experiment, we define a time-evolution operator of the nonunitary quantum walk with gain and loss so that one can flexibly tune various parameters of the system, while the basic setup of the system should not be altered. At first, we introduce the time-evolution operator of the 1D two-step unitary quantum walk, and then extend it

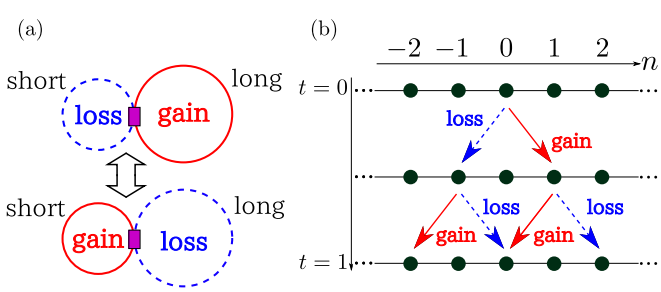

FIG. 1. (a) Experimental setup. Optical pulses corresponding to walkers go around in two optical-fiber loops with different circumferences, and they are split into two at the connected point (shown by a rectangle) corresponding to coin operators. After a single cycle, pulses are delayed or advanced in time due to the difference of lengths of two fiber loops, corresponding to shift operators. The time evolution of the single time step is composed of the following two substeps. At the former half of the step, amplitudes of pulses passing through the long (short) loop are amplified (dumped) and, at the latter half of the step, vice versa. (b) Translation from the above description to the standard schematic view of the 1D two-step quantum walk. When a pulse passes the long (short) loop and it is delayed (advanced) in time, this is interpreted as that the walker "shifts to the right (left)." In both (a) and (b), loops or arrows with gain (loss) are depicted in solid (dashed) lines.

to the nonunitary one. We introduce the basis of the walker's 1D position space $|n\rangle$ and internal states $|L\rangle = (1,0)^T, |R\rangle = (0,1)^T$, where the superscript T denotes the transpose. The symbols L, R represent the walker's internal states, say, left mover and right mover components, respectively. The time-evolution operator of the two-step unitary quantum walk U_u is defined as

$$U_u = S\,C(\theta_2)\,S\,C(\theta_1).$$

Here, the coin operator $C(\theta_i)$, where the subscript $i = 1$ or 2 distinguishes the parameter for the first or second coin operators, respectively, and the shift operator S are standard elemental operators of quantum walks defined as

$$C(\theta_i) = \sum_n |n\rangle\langle n| \otimes \tilde{C}(\theta_{i,n}), \tag{1a}$$

$$\tilde{C}(\theta_{i,n}) = \begin{pmatrix} \cos[\theta_i(n)] & i\sin[\theta_i(n)] \\ i\sin[\theta_i(n)] & \cos[\theta_i(n)] \end{pmatrix}, \tag{1b}$$

and

$$S = \sum_n \begin{pmatrix} |n-1\rangle\langle n| & 0 \\ 0 & |n+1\rangle\langle n| \end{pmatrix}. \tag{2}$$

Since $\tilde{C}(\theta_{i,n})$ acts on the internal states of walkers at the position n, the coin operator $C(\theta_i)$ mixes the walker's internal states, where the value of $\theta_i(n)$ determines how strongly to mix at each position n. The shift operator S changes the position of walkers depending on the internal states. Note that, in the present work, we follow a rule that an operator with a tilde on the top acts on the space of internal states of walkers.

With an initial state $|\psi(0)\rangle$, the wave function after the t time step is described as

$$|\psi(t)\rangle = U^t|\psi(0)\rangle = \sum_{n,\sigma=L,R} \psi_{n,\sigma}(t)\,|n\rangle \otimes |\sigma\rangle.$$

From the eigenvalue equation, we define the quasienergy ε as

$$U|\Psi_\lambda\rangle = \lambda|\Psi_\lambda\rangle, \quad \lambda = e^{-i\varepsilon},$$

where $|\Psi_\lambda\rangle$ is the eigenvector with the eigenvalue λ. For the unitary quantum walk, λ should satisfy $|\lambda| = 1$ and then ε should be real with 2π periodicity.

The unitary quantum walk described by U_u can be extended to the nonunitary one described by

$$U = S\,G_2\,\Phi_2\,C(\theta_2)\,S\,G_1\,\Phi_1\,C(\theta_1), \tag{3}$$

which is consistent with the basic experimental setup in Ref. [45]. Here, we introduce additional elemental operators: the gain and/or loss (gain-loss) operator G_i and the phase operator Φ_i defined as

$$G_i = \sum_n |n\rangle\langle n| \otimes \tilde{G}_{i,n}, \quad \tilde{G}_{i,n} = \begin{pmatrix} g_{i,L}(n) & 0 \\ 0 & g_{i,R}(n) \end{pmatrix}, \tag{4}$$

$$\Phi_i = \sum_n |n\rangle\langle n| \otimes \tilde{\Phi}_{i,n}, \quad \tilde{\Phi}_{i,n} = \begin{pmatrix} e^{i\phi_{i,L}(n)} & 0 \\ 0 & e^{i\phi_{i,R}(n)} \end{pmatrix}, \tag{5}$$

respectively. The gain-loss operator G_i multiplies the wave function amplitude $\psi_{n,\sigma}(t)$ by the factor $g_{i,\sigma}(n)$. If $g_{i,\sigma}(n) \neq 1$,

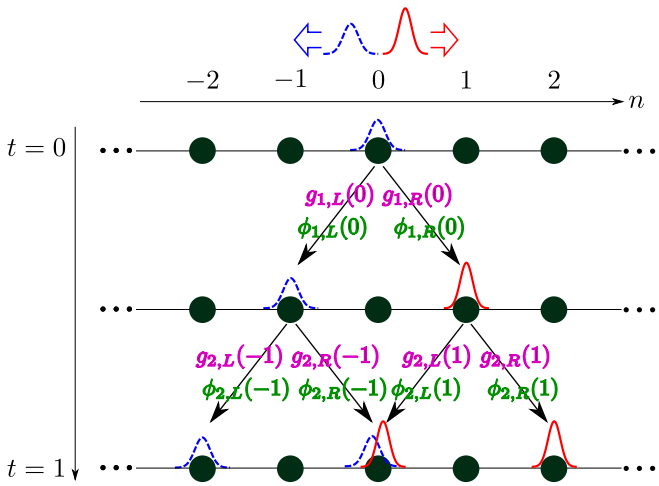

FIG. 2. An example of the one time step of time evolution described by the time-evolution operator U with the initial state $|\psi(0)\rangle = |0,L\rangle$. The left (right) mover components are depicted as waves in dashed (solid) curves. At each time step, on a site n, the left (right) mover component $\psi_{n,L(R)}(t)$ is varied to the linear combination of $\psi_{n,L}(t)$ and $\psi_{n,R}(t)$ by the coin operator $C(\theta_i)$. Then, left mover components $\psi_{n,L}(t)$ move to the left and right mover components $\psi_{n,R}(t)$ move to the right by the shift operator S. During walkers changing their positions, they are affected by gain or loss of the amplitude and phase modulation; that is, $\psi_{n,\sigma}(t)$ increases or decreases by the factor $g_{i,\sigma}(n)$ by the gain-loss operator G_i, and earns the phase $\phi_{i,\sigma}(n)$ by the phase operator Φ_i.

then G_i and U become nonunitary operators. The phase operator Φ_i adds the phase $\phi_{i,\sigma}(n)$ to that of the wave function amplitude $\psi_{n,\sigma}(t)$. The time evolution of a walker described by U is schematically explained in Fig. 2. Thereby, the time-evolution operator of the nonunitary quantum walk contains three kinds of n-dependent parameters, $\theta_i(n), g_{i,\sigma}(n)$, and $\phi_{i,\sigma}(n)$. The setup in the experiment in Ref. [45] is realized with the parameters in Eq. (39), as we discuss in Sec. IV.

III. $\mathcal{PT}$ AND EXTRA SYMMETRIES OF THE NONUNITARY QUANTUM WALK

In this section, we identify various symmetries embedded in the time-evolution operator of the nonunitary quantum walk in Eq. (3). Among them, our main target is $\mathcal{PT}$ symmetry, which can restrict the quasienergy of the nonunitary quantum walk to real numbers. To begin with, let us summarize the argument on the $\mathcal{PT}$ symmetry of Hamiltonians [4]. In order to define $\mathcal{PT}$ symmetry, we consider parity symmetry and TRS at first. For a system described by a (Hermitian or non-Hermitian) Hamiltonian H, it is required that the Hamiltonian satisfies the following relations to retain parity symmetry and TRS:

$$\mathcal{P}H\mathcal{P}^{-1} = H, \tag{6}$$

$$\mathcal{T}H\mathcal{T}^{-1} = H, \tag{7}$$

respectively. Here, the parity-symmetry operator $\mathcal{P}$, which flips the sign of position from n to $-n$, is a unitary operator and does not include complex conjugation $\mathcal{K}$. The TRS operator $\mathcal{T}$, which inverts the direction of time from t to $-t$, is an antiunitary operator including $\mathcal{K}$. By combing Eqs. (6) and (7), $\mathcal{PT}$ symmetry of the Hamiltonian is defined as

$$(\mathcal{PT})H(\mathcal{PT})^{-1} = H, \tag{8}$$

where the combined symmetry operator $\mathcal{PT}$ is the antiunitary operator.

When the Hamiltonian satisfies both Eqs. (6) and (7), the relation for $\mathcal{PT}$ symmetry (8) is automatically satisfied. However, even when the Hamiltonian has neither parity symmetry [Eq. (6)] nor TRS [Eq. (7)], it can satisfy Eq. (8) to establish $\mathcal{PT}$ symmetry. This recovering of $\mathcal{PT}$ symmetry becomes much important in the case of non-Hermitian Hamiltonians, since one of the standard ways to phenomenologically include the effects of gain and loss is adding non-Hermitian imaginary potential terms into a Hermitian Hamiltonian, which prevents retaining TRS in Eq. (7) due to complex conjugation $\mathcal{K}$. In addition to the presence of $\mathcal{PT}$ symmetry of the non-Hermitian Hamiltonian, we demand that eigenvectors of the non-Hermitian Hamiltonian are also eigenvectors of the $\mathcal{PT}$-symmetry operator,

$$H|\Psi_\lambda\rangle = E_\lambda|\Psi_\lambda\rangle, \quad \mathcal{PT}|\Psi_\lambda\rangle = e^{i\delta}|\Psi_\lambda\rangle, \tag{9}$$

where the phase δ is a real number. Satisfying both conditions Eqs. (8) and (9) establishes the sufficient condition that the eigenenergy E_λ is kept to be a real number even for the non-Hermitian Hamiltonian. Hereafter, we apply the above argument to the time-evolution operator of nonunitary quantum walks.

A. Symmetries in homogeneous systems

For simplicity, at first, we assume the homogeneous nonunitary quantum walk in which all parameters have no position n dependencies, so that we can treat operators in momentum space by applying the Fourier transformation.

In the homogeneous systems, the operators $C(\theta_i), G_i$, and Φ_i are diagonal in the momentum representation, and we can drop the subscript n from $\tilde{C}(\theta_{i,n}), \tilde{G}_{i,n}$, and $\tilde{\Phi}_{i,n}$. For further simplification, we assume

$$\tilde{G}_2 = \tilde{G}_1^{-1} = \tilde{G} = \begin{pmatrix} e^{\gamma} & 0 \\ 0 & e^{-\gamma} \end{pmatrix} = e^{\gamma\sigma_3}, \tag{10}$$

$$\tilde{\Phi}_2 = \tilde{\Phi}_1 = \tilde{\Phi} = \begin{pmatrix} e^{i\phi} & 0 \\ 0 & e^{-i\phi} \end{pmatrix} = e^{i\phi\sigma_3}, \tag{11}$$

where $\sigma_{j=1,2,3}$ are Pauli matrices. [The peculiar choice of $\tilde{G}_2 = \tilde{G}_1^{-1}$ is motivated by the setup of the experiment [45] as shown in Eqs. (39b) and (39c).] By using the Pauli matrix σ_1, the coin operator is also written as

$$\tilde{C}(\theta_i) = \begin{pmatrix} \cos[\theta_i] & i\sin[\theta_i] \\ i\sin[\theta_i] & \cos[\theta_i] \end{pmatrix} = e^{i\theta_i\sigma_1}. \tag{12}$$

With the Fourier transformation, the shift operator in Eq. (2) can be rewritten as

$$S = \sum_k |k\rangle\langle k| \otimes \tilde{S}(k), \quad \tilde{S}(k) = \begin{pmatrix} e^{+ik} & 0 \\ 0 & e^{-ik} \end{pmatrix} = e^{ik\sigma_3}, \tag{13}$$

where k stands for the wave number. Accordingly, the time-evolution operator U in Eq. (3) in the momentum representation is written down as

$$U = \sum_k |k\rangle\langle k| \otimes \tilde{U}(k), \tag{14a}$$

$$\tilde{U}(k) = \tilde{S}(k)\,\tilde{G}\,\tilde{\Phi}\,\tilde{C}(\theta_2)\,\tilde{S}(k)\,\tilde{G}^{-1}\,\tilde{\Phi}\,\tilde{C}(\theta_1). \tag{14b}$$

Since determinants of all the above elemental operators are one, the determinant of the time-evolution operator $\tilde{U}(k)$ is also one, while the operator is nonunitary when $\gamma \neq 0$.

By solving the eigenvalue problem, the quasienergy of the time-evolution operator in Eq. (14b) is derived as

$$\cos(\pm\varepsilon) = \cos\theta_1 \cos\theta_2 \cos 2(k+\phi) - \sin\theta_1 \sin\theta_2 \cosh(2\gamma), \tag{15}$$

and the corresponding eigenvector is

$$|\Psi_{k,\pm}\rangle = e^{-i\frac{\theta_1}{2}\sigma_1} \frac{e^{-i\eta_k}}{2\sqrt{\cos 2\xi_k}} \begin{pmatrix} e^{i\alpha} \pm e^{-i\alpha} \\ -i[e^{i\alpha} \mp e^{-i\alpha}] \end{pmatrix}, \tag{16}$$

$$\alpha = \eta_k \pm \xi_k,$$

where η_k and ξ_k are defined as

$$\tan(2\eta_k) = d_1/d_3,$$

$$\cos(2\xi_k) = \sqrt{1-(d_2/|d_k|)^2}, \quad \sin(2\xi_k) = d_2/|d_k|,$$

$$|d_k| = |d_3 + i d_1|,$$

$$d_1 = \sin\theta_1 \cos\theta_2 \cos 2(k+\phi) + \cos\theta_1 \sin\theta_2 \cosh(2\gamma),$$

$$d_2 = -\sin\theta_2 \sinh(\pm 2\gamma),$$

$$d_3 = -\cos\theta_2 \sin 2(k+\phi).$$

We remark that, while η_k is always real, ξ_k becomes imaginary when $d_2^2 > d_1^2 + d_3^2$. Figure 3 shows the quasienergy as a function of k with several values of γ: (a) $e^\gamma = 1$, (b) $e^\gamma = 1.1$, (c) $e^\gamma = 1.34\ldots$, and (d) $e^\gamma = 1.5$ (see the caption of Fig. 3 for other parameters). Comparing with the case of the unitary quantum walk in Fig. 3(a), we see from Fig. 3(b) that, while the quasienergy gap around $\varepsilon = 0$ becomes narrow, the quasienergy remains entirely real even for the finite γ (nonunitary quantum walks). This keeps holding as long as the absolute value of the right-hand side in Eq. (15) does not exceed one, which is consistent with the condition to keep ξ_k real. The value of γ used for Fig. 3(c) corresponds to this limit and the quasienergy gap closes at $\varepsilon = 0$, the so-called exceptional point [5]. When γ exceeds this value, part of the quasienergy whose components of real number are zero exhibits finite values of imaginary number, as shown in Fig. 3(d). These observations suggest the presence of $\mathcal{PT}$ symmetry or more generalized symmetries in Refs. [53–55]. Henceforth, we show that there exists $\mathcal{PT}$ symmetry, as Ref. [45] has stated. In addition, from Eq. (15), we also understand that the quasienergy becomes symmetric with respect to $\varepsilon = 0$. Indeed, these properties can be understood

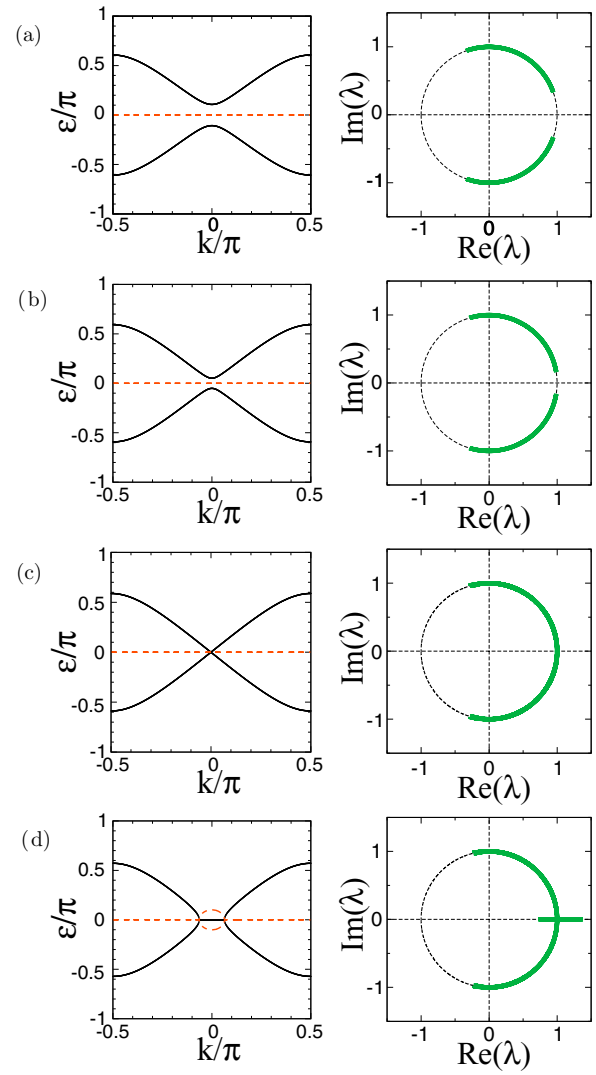

FIG. 3. The quasienergy in Eq. (15) with various gain-loss parameters when $\theta_1 = \pi/4$, $\theta_2 = -\pi/7$, and $\phi = 0$. The left column shows the quasienergy as a function of k where the solid (dashed) curves represent the real (imaginary) part of the quasienergy, while the right column shows the eigenvalue on a unit circle indicating $|\lambda| = 1$ on a complex plain. (a) In the case of $e^\gamma = 1$, all of the quasienergies are real as the time-evolution operator is unitary. (b) In the case of $e^\gamma = 1.3$, the quasienergy is entirely real although the time-evolution operator is nonunitary, and quasienergy gaps around $\varepsilon = 0,\pi$ open. (c) In the case of $e^\gamma = \exp\{\cosh^{-1}[(\cos\theta_1\cos\theta_2 - 1)/(\sin\theta_1\sin\theta_2)]/2\} = 1.34\ldots$, while the quasienergy is entirely real, the quasienergy gap around $\varepsilon = 0$ closes. (d) In the case of $e^\gamma = 1.5$, the quasienergy becomes complex for $|k|/\pi \lesssim 0.1$, and the gap closes.

from symmetries embedded in the nonunitary time-evolution operator in Eq. (14), which is also shown in the following subsections.

1. $\mathcal{PT}$ symmetry

We introduce the parity symmetry and TRS operators, $\mathcal{P}$ and $\mathcal{T}$, in the position and momentum representations as

follows;

$$\mathcal{P} = \sum_n |-n\rangle\langle n| \otimes \tilde{\mathcal{P}} = \sum_k |-k\rangle\langle k| \otimes \tilde{\mathcal{P}}, \tag{17}$$

$$\mathcal{T} = \sum_n |n\rangle\langle n| \otimes \tilde{\mathcal{T}} = \sum_k |-k\rangle\langle k| \otimes \tilde{\mathcal{T}}, \tag{18}$$

where $\tilde{\mathcal{P}}$ and $\tilde{\mathcal{T}}$ act on the internal space of the time-evolution operator. We understand that the parity-symmetry operator $\mathcal{P}$ flips the sign of momentum k because the operator $\mathcal{P}$ changes the position n to $-n$ and the TRS operator $\mathcal{T}$ also flips the sign of k since the operator $\mathcal{T}$ is an antiunitary operator including a complex conjugation $\mathcal{K}$.

Then, we convert Eqs. (6)–(8) for the Hamiltonian into those for the time-evolution operator in Eq. (14). By using the relation between the time-evolution operator and the effective Hamiltonian $U = e^{-iH}$, we derive relations for parity symmetry, TRS, and $\mathcal{PT}$ symmetry as

$$\mathcal{P}U\mathcal{P}^{-1} = U,$$
$$\mathcal{T}U\mathcal{T}^{-1} = U^{-1},$$
$$(\mathcal{PT})U(\mathcal{PT})^{-1} = U^{-1}.$$

By substituting Eqs. (17) and (18) into the above relations, we obtain

$$\tilde{\mathcal{P}}\tilde{U}(k)\tilde{\mathcal{P}}^{-1} = \tilde{U}(-k), \tag{19}$$

$$\tilde{\mathcal{T}}\tilde{U}(k)\tilde{\mathcal{T}}^{-1} = \tilde{U}^{-1}(-k), \tag{20}$$

$$(\tilde{\mathcal{P}}\tilde{\mathcal{T}})\tilde{U}(k)(\tilde{\mathcal{P}}\tilde{\mathcal{T}})^{-1} = \tilde{U}^{-1}(+k), \tag{21}$$

respectively.

In order to identify symmetries, we need to examine whether the time-evolution operator of the nonunitary quantum walk in Eq. (14b) satisfies the above relations. For parity symmetry in Eq. (19), on one hand, we can straightforwardly obtain relations for the same elemental operators by comparing the left and right hand sides of Eq. (19) by substituting Eq. (14b), e.g., $\tilde{\mathcal{P}}\tilde{S}(k)\tilde{\mathcal{P}}^{-1} = \tilde{S}(-k), \tilde{\mathcal{P}}\tilde{G}\tilde{\mathcal{P}}^{-1} = \tilde{G}$, and etc. On the other hand, for TRS and $\mathcal{PT}$ symmetry, there appear the inverse operators of the time-evolution operator on the right-hand side of Eqs. (20) and (21), which invert the time order of elemental operators and then prevent us from deriving the one to one correspondence for the same elemental operators. Indeed, according to recent work on symmetries which are important to topological phases of quantum walks, it has become clear that the presence of the inverse of time-evolution operators in symmetry relations prevents us from straightforwardly identifying the symmetries. To overcome this difficulty, the concept of *symmetry time frame* has been introduced [48]. The symmetry time frame requires a redefinition of the time-evolution operator by shifting the origin of time so that the time-evolution operator exhibits symmetric order of elemental operators in the time direction. In the case of $\tilde{U}(k)$ in Eq. (14b), the redefined time-evolution operator $\tilde{U}'(k)$ fitted in the symmetric time frame is written down as

$$\tilde{U}'(k) = \tilde{C}(\theta_1/2)\,\tilde{S}(k)\,\tilde{\Phi}\,\tilde{G}\,\tilde{C}(\theta_2)\,\tilde{G}^{-1}\,\tilde{\Phi}\,\tilde{S}(k)\,\tilde{C}(\theta_1/2), \tag{22}$$

which we can obtain by the unitary transformation $\tilde{U}'(k) = e^{i\frac{\theta_1}{2}\sigma_1}\tilde{U}(k)e^{-i\frac{\theta_1}{2}\sigma_1}$. Here, we use the commutative property between operators $\tilde{G}, \tilde{S}(k)$, and $\tilde{\Phi}$ as they are described by exponentials of σ_3. By substituting $\tilde{U}'(k)$ in Eq. (22) into Eqs. (19)–(21), we obtain conditions for elemental operators $\tilde{C}(\theta_i), \tilde{G}, \tilde{S}(k)$, and $\tilde{\Phi}$ to retain each symmetry. For example, in the case of TRS, we obtain the following two equations from the left and right hand sides of Eq. (20) by substituting Eq. (22):

$$\text{LHS} = [\tilde{\mathcal{T}}\tilde{C}(\theta_1/2)\tilde{\mathcal{T}}^{-1}][\tilde{\mathcal{T}}\tilde{S}(k)\tilde{\mathcal{T}}^{-1}][\tilde{\mathcal{T}}\tilde{\Phi}\tilde{\mathcal{T}}^{-1}][\tilde{\mathcal{T}}\tilde{G}\tilde{\mathcal{T}}^{-1}]\cdots,$$

$$\text{RHS} = [\tilde{C}^{-1}(\theta_1/2)][\tilde{S}^{-1}(-k)][\tilde{\Phi}^{-1}][\tilde{G}]\cdots.$$

Comparing the two equations, we obtain conditions for the elemental operators, such as $\tilde{\mathcal{T}}\tilde{C}(\theta_1)\tilde{\mathcal{T}}^{-1} = \tilde{C}^{-1}(\theta_1)$, and so on. We summarize conditions on all elemental operators for various symmetries in Table I. Using Table I, we discuss symmetries of the time-evolution operator by starting from the unitary case, then including the gain-loss and phase operators step by step.

The case $\gamma = \phi = 0$. In this case, the time-evolution operator $\tilde{U}'(k)$ describes the unitary quantum walk and we consider conditions only on $\tilde{C}(\theta_i)$ and $\tilde{S}(k)$ in Table I. From the anticommutation relations of Pauli matrices, we identify that $\tilde{U}'(k)$ satisfies parity symmetry and TRS with the following symmetry operators:

$$\tilde{\mathcal{P}} = \sigma_1, \quad \tilde{\mathcal{T}} = \sigma_1\mathcal{K}. \tag{23}$$

Therefore, by combing the two symmetry operators in Eq. (23), the $\mathcal{PT}$-symmetry operator is determined as

$$\tilde{\mathcal{P}}\tilde{\mathcal{T}} = \sigma_0\mathcal{K}, \tag{24}$$

where $\sigma_0 = \text{diag}(1,1)$, and $\tilde{U}'(k)$ also possesses $\mathcal{PT}$ symmetry.

The case $\gamma \neq 0$ *and* $\phi = 0$. The finite γ makes $\tilde{U}'(k)$ the nonunitary time-evolution operator and we should consider the additional condition on the gain-loss operator $\tilde{G}$ as well as those on $\tilde{C}(\theta_i)$ and $\tilde{S}(k)$ in Table I. Since conditions on $\tilde{G}$ for parity symmetry and TRS by symmetry operators in Eq. (23) are not satisfied, the time-evolution operator $\tilde{U}'(k)$ has neither parity symmetry nor TRS. However, when we consider $\mathcal{PT}$ symmetry, the condition $(\tilde{\mathcal{P}}\tilde{\mathcal{T}})\tilde{G}(\tilde{\mathcal{P}}\tilde{\mathcal{T}})^{-1} = \tilde{G}$ with $\tilde{\mathcal{P}}\tilde{\mathcal{T}}$ in Eq. (24) is satisfied. Therefore, we identify $\mathcal{PT}$ symmetry and confirm that the nonunitary time-evolution operator $\tilde{U}'(k)$ (with $\phi = 0$) preserves $\mathcal{PT}$ symmetry.

The case $\gamma \neq 0$ *and* $\phi \neq 0$. Now, the condition on the phase operator in Table I is also maintained to retain $\mathcal{PT}$ symmetry. We easily confirm the condition $(\tilde{\mathcal{P}}\tilde{\mathcal{T}})\tilde{\Phi}(\tilde{\mathcal{P}}\tilde{\mathcal{T}})^{-1} = \tilde{\Phi}^*$ with $\tilde{\mathcal{P}}\tilde{\mathcal{T}}$ in Eq. (24). Thereby, we conclude that, nevertheless, individual parity symmetry and TRS are broken in the nonunitary quantum walk with the phase operator in the homogeneous system; there $\mathcal{PT}$ symmetry is present.

We recall that the sufficient condition for quasienergy being real requires the other condition, namely, that the eigenvector of the nonunitary time-evolution operator is also one of the $\mathcal{PT}$-symmetry operator. To check this, applying the unitary transformation $e^{i(\theta_1/2)\sigma_1}$ to the eigenvector of $\tilde{U}(k)$ in Eq. (16), the eigenvector of $\tilde{U}'(k)$ fitted in the symmetry time frame is described as $|\Psi'_{k,\pm}\rangle = e^{i(\theta_1/2)\sigma_1}|\Psi_{k,\pm}\rangle$. Then, we can

TABLE I. A list of conditions for elemental operators so that the time-evolution operator $\tilde{U}'(k)$ satisfies parity, time-reversal, and $\mathcal{PT}$, as well as chiral, particle-hole, and parity-chiral symmetries. The first column indicates each symmetry, the second column represents the symmetry operators $\tilde{X} = \tilde{\mathcal{P}}, \tilde{\mathcal{T}}, \tilde{\mathcal{P}}\tilde{\mathcal{T}}, \tilde{\Gamma}, \tilde{\Xi}$, and $\tilde{\mathcal{P}}\tilde{\Gamma}$, and the third column $\tilde{X}_u$ shows specific forms of symmetry operators which are derived from the unitary time-evolution operator with $\gamma = \phi = 0$. The fourth to seventh columns show conditions for the elemental operators to satisfy each symmetry. This part of the table should be read according to the following example: in order to satisfy parity symmetry the coin operator should satisfy $\tilde{\mathcal{P}}\tilde{C}(\theta_i)\tilde{\mathcal{P}}^{-1} = \tilde{C}(\theta_i)$. The [yes] or [no] next to each condition explains whether the condition is satisfied or not with the symmetry operator $\tilde{X}_u$. Note that $\tilde{C}(\theta_i) = e^{i\theta_i\sigma_1}$, $\tilde{S}(k) = e^{ik\sigma_3}$, $\tilde{G} = e^{\gamma\sigma_3}$, and $\tilde{\Phi} = e^{i\phi\sigma_3}$. We use the following relations: $\tilde{C}^{-1}(\theta_i) = \tilde{C}(-\theta_i)$, $\tilde{S}^{-1}(k) = \tilde{S}(-k)$, $\tilde{S}^{-1}(-k) = \tilde{S}(+k)$, and $\tilde{\Phi}^{-1} = \tilde{\Phi}^*$.

Symmetry	$\tilde{X}$	$\tilde{X}_u$	$\tilde{X}\tilde{C}(\theta_i)\tilde{X}^{-1}$	$\tilde{X}\tilde{S}(k)\tilde{X}^{-1}$	$\tilde{X}\tilde{G}\tilde{X}^{-1}$	$\tilde{X}\tilde{\Phi}\tilde{X}^{-1}$
Parity symmetry	$\tilde{\mathcal{P}}$	σ_1	$\tilde{C}(+\theta_i)$ [yes]	$\tilde{S}(-k)$ [yes]	$\tilde{G}$ [no]	$\tilde{\Phi}$ [no]
Time-reversal symmetry (TRS)	$\tilde{\mathcal{T}}$	$\sigma_1\mathcal{K}$	$\tilde{C}(-\theta_i)$ [yes]	$\tilde{S}(+k)$ [yes]	$\tilde{G}$ [no]	$\tilde{\Phi}^*$ [no]
$\mathcal{PT}$ symmetry	$\tilde{\mathcal{P}}\tilde{\mathcal{T}}$	$\sigma_0\mathcal{K}$	$\tilde{C}(-\theta_i)$ [yes]	$\tilde{S}(-k)$ [yes]	$\tilde{G}$ [yes]	$\tilde{\Phi}^*$ [yes]
Chiral symmetry	$\tilde{\Gamma}$	$i\sigma_2$	$\tilde{C}(-\theta_i)$ [yes]	$\tilde{S}(-k)$ [yes]	$\tilde{G}$ [no]	$\tilde{\Phi}^*$ [yes]
Particle-hole symmetry (PHS)	$\tilde{\Xi}$	$\sigma_3\mathcal{K}$	$\tilde{C}(+\theta_i)$ [yes]	$\tilde{S}(-k)$ [yes]	$\tilde{G}$ [yes]	$\tilde{\Phi}$ [no]
Parity-chiral symmetry (PCS)	$\tilde{\mathcal{P}}\tilde{\Gamma}$	σ_3	$\tilde{C}(-\theta_i)$ [yes]	$\tilde{S}(+k)$ [yes]	$\tilde{G}$ [yes]	$\tilde{\Phi}^*$ [no]

straightforwardly confirm the equation

$$\tilde{\mathcal{P}}\tilde{\mathcal{T}}|\Psi'_{k,\pm}\rangle = \pm e^{+i2\eta_k}|\Psi'_{k,\pm}\rangle,$$

as long as ξ_k is real (then ε is also real). Therefore, we confirm that the entirely real quasienergy in Eq. (15) originates in the $\mathcal{PT}$ symmetry of the nonunitary time-evolution operator.

2. *Extra symmetries*

The time-evolution operator of the nonunitary quantum walk in Eq. (22) can possess extra symmetries. Here, we discuss such symmetries which are intensively studied for topological phases of the quantum walk [44,48–52]. These extra symmetries are chiral symmetry and particle-hole symmetry (PHS) defined for a Hamiltonian H as

$$\Gamma\, H\, \Gamma^{-1} = -H, \tag{25}$$

$$\Xi\, H\, \Xi^{-1} = -H, \tag{26}$$

respectively. The chiral-symmetry operator Γ is a unitary operator, while the PHS operator Ξ is an antiunitary one. These two symmetries guarantee that the system has a pair of eigenstates with opposite sign of eigenvalues if the eigenvalue is real. Accordingly, eigenenergy appears symmetric with respect to zero energy. Following the same procedure as before, we convert Eqs. (25) and (26) to symmetry relations for the time-evolution operator:

$$\Gamma\, U\, \Gamma^{-1} = U^{-1},$$

$$\Xi\, U\, \Xi^{-1} = U.$$

Defining the symmetry operators as

$$\Gamma = \sum_n |n\rangle\langle n| \otimes \tilde{\Gamma} = \sum_k |k\rangle\langle k| \otimes \tilde{\Gamma},$$

$$\Xi = \sum_n |n\rangle\langle n| \otimes \tilde{\Xi} = \sum_k |-k\rangle\langle k| \otimes \tilde{\Xi},$$

we derive relations to retain chiral symmetry and PHS:

$$\tilde{\Gamma}\, \tilde{U}(k)\, \tilde{\Gamma}^{-1} = \tilde{U}^{-1}(+k), \tag{27}$$

$$\tilde{\Xi}\, \tilde{U}(k)\, \tilde{\Xi}^{-1} = \tilde{U}(-k). \tag{28}$$

Substituting Eq. (22) into Eqs. (27) and (28), we again obtain conditions on the elemental operators to retain chiral symmetry and PHS as shown in Table I. Due to 2π periodicity of the quasienergy, if the time-evolution operator satisfies Eq. (27) and/or (28), the quasienergy appears symmetric with respect to $\varepsilon = 0$ and π.

The case $\gamma = \phi = 0$. At first, we focus on conditions on the coin and shift operators in the case of chiral symmetry in Table I for this unitary quantum walk. We find that, with the symmetry operator $\tilde{\Gamma} = i\sigma_2$, chiral symmetry is retained. It is known that if TRS and chiral symmetry are presented, PHS is simultaneously retained with the symmetry operator $\tilde{\Xi} = \tilde{\Gamma}\tilde{\mathcal{T}}$. In summary, by using

$$\tilde{\Gamma} = i\sigma_2, \quad \tilde{\Xi} = \sigma_3\mathcal{K}, \tag{29}$$

the unitary time-evolution operator $\tilde{U}'(k)$ has extra symmetries, chiral symmetry, and PHS.

The case $\gamma \neq 0$ *and* $\phi = 0$. In order to retain chiral symmetry and PHS for this nonunitary quantum walk, the gain-loss operator $\tilde{G}$ should be unchanged ($\tilde{X}\tilde{G}\tilde{X}^{-1} = \tilde{G}$) when $\tilde{X} = \tilde{\Gamma}$ or $\tilde{\Xi}$ in Eq. (29) is acted on. We understand that $\tilde{X} = \tilde{\Xi}$ keeps $\tilde{G}$ as is, while $\tilde{X} = \tilde{\Gamma}$ does not. Thereby, only PHS survives after including gain and loss effects. However, we can introduce a new symmetry combined with parity and chiral symmetries,

$$(\mathcal{P}\Gamma)\, U\, (\mathcal{P}\Gamma)^{-1} = U^{-1},$$

which we call parity-chiral symmetry (PCS). Taking account of Eqs. (19) and (27), we derive the symmetry relation for PCS,

$$(\tilde{\mathcal{P}}\tilde{\Gamma})\, \tilde{U}(k)\, (\tilde{\mathcal{P}}\tilde{\Gamma})^{-1} = \tilde{U}^{-1}(-k), \tag{30}$$

and then obtain conditions on each elemental operator as listed in Table I. We note that PCS also guarantees the symmetric behavior of the quasienergy with respect to $\varepsilon = 0$ and π. From Eqs. (23) and (29), the PCS operator becomes

$$\tilde{\mathcal{P}}\tilde{\Gamma} = \sigma_3, \tag{31}$$

(we ignore an unimportant minus sign). With the above symmetry operator $\tilde{\mathcal{P}}\tilde{\Gamma}$, we confirm that $\tilde{U}'(k)$ possesses PCS,

and the symmetric property of the quasienergy is guaranteed by PHS and PCS.

The case $\gamma \neq 0$ and $\phi \neq 0$. Finally, we consider the nonunitary quantum walk with finite phases whose quasienergy is given in Eq. (15). To retain PHS and PCS, the phase operator should satisfy $\tilde{\Xi}\tilde{\Phi}\tilde{\Xi}^{-1} = \tilde{\Phi}$ and $(\tilde{\mathcal{P}}\tilde{\Gamma})\tilde{\Phi}(\tilde{\mathcal{P}}\tilde{\Gamma})^{-1} = \tilde{\Phi}^*$, respectively. However, both conditions are not satisfied with the symmetry operators in Eqs. (29) and (31). Thereby, the finite γ and ϕ break all symmetries which guarantee a pair of eigenstates with the opposite quasienergies.

While the above result implies that the pair of quasienergies in Eq. (15) does not originate in symmetry, we can still find the contributions of symmetry by introducing a modified version of parity symmetry defined below. Because of translation symmetry in the homogeneous system, we reexpress the time-evolution operator in Eq. (22) by including the phase operator into the shift operator as

$$\tilde{U}'(k) = \tilde{C}(\theta_1/2)\,\tilde{S}(k+\phi)\,\tilde{G}\,\tilde{C}(\theta_2)\,\tilde{G}^{-1}\,\tilde{S}(k+\phi)\,\tilde{C}(\theta_1/2). \tag{32}$$

Next, we introduce the modified parity-symmetry operator with phase modulations defined as

$$\mathcal{P}_\phi = \sum_n e^{-i2\phi n}|-n\rangle\langle n| \otimes \tilde{\mathcal{P}}_\phi = \sum_k |-k-2\phi\rangle\langle k| \otimes \tilde{\mathcal{P}}_\phi.$$

By combing the modified parity-symmetry operator $\mathcal{P}_\phi$ and chiral-symmetry operator Γ, the condition on the shift operator $\tilde{S}(k+\phi)$ to retain modified PCS, $(\tilde{\mathcal{P}}_\phi\tilde{\Gamma})\tilde{U}'(k)(\tilde{\mathcal{P}}_\phi\tilde{\Gamma})^{-1} = \tilde{U}'^{-1}(-k-2\phi)$, becomes

$$(\tilde{\mathcal{P}}_\phi\tilde{\Gamma})\tilde{S}(k+\phi)(\tilde{\mathcal{P}}_\phi\tilde{\Gamma})^{-1} = \tilde{S}(k+\phi),$$

which is satisfied by the symmetry operator $\tilde{\mathcal{P}}_\phi\tilde{\Gamma} = \sigma_3$. Note that conditions for $\tilde{C}(\theta_i)$ and $\tilde{G}$ to retain modified PCS are the same with those of PCS, since both operators are k independent. Thereby, we identify that the pair of quasienergies in Eq. (15) originates from modified PCS.

B. Symmetries in inhomogeneous systems

Next, we consider $\mathcal{PT}$ symmetry, PHS, and PCS of the time-evolution operator of the nonunitary quantum walk in Eq. (3) with position-dependent parameters. Therefore, we need to consider the time-evolution operator in the position representation. Taking the symmetry operators for internal space in Eqs. (24), (29), and (31) into account, those in the position representation are described as

$$\mathcal{PT} = \sum_n |-n+q\rangle\langle n| \otimes \sigma_0\mathcal{K}, \tag{33a}$$

$$\Xi = \sum_n |n\rangle\langle n| \otimes \sigma_3\mathcal{K}, \tag{33b}$$

$$\mathcal{P}\Gamma = \sum_n |-n+q\rangle\langle n| \otimes \sigma_3, \tag{33c}$$

where the index q is introduced to determine the origin of the space reflection point (see Fig. 4) because we treat lattice systems. By using the symmetry operators in Eqs. (33a)–(33c),

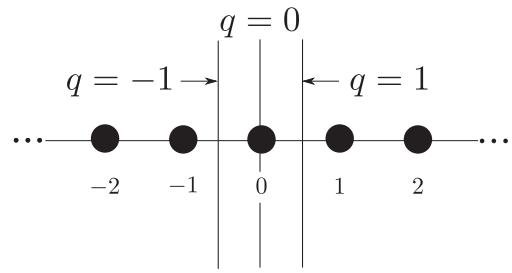

FIG. 4. The difference of the reflection points of the parity-symmetry operator. When $q = 0$, the reflection point is on the site $n = 0$. When $q = \pm 1$, the reflection point is between sites $n = 0$ and $n = \pm 1$.

each symmetry defined for the time-evolution operator in the position representation becomes

$$(\mathcal{PT})U(\mathcal{PT})^{-1} = U^{-1}, \tag{34a}$$

$$\Xi U \Xi^{-1} = U, \tag{34b}$$

$$(\mathcal{P}\Gamma)U(\mathcal{P}\Gamma)^{-1} = U^{-1}. \tag{34c}$$

Equations (33) and (34) guarantee that if two of the above three symmetries are confirmed, there also exists the other symmetry which is derived by combining the confirmed two symmetries. Even in the position representation, we need to use the time-evolution operator fitted into the symmetry time frame written as

$$U' = C(\theta_1/2)\,S\,G_2\,\Phi_2\,C(\theta_2)\,S\,G_1\,\Phi_1\,C(\theta_1/2). \tag{35}$$

As shown in Sec. III A, when parameters of the coin, gain-loss, and phase operators are position independent, conditions to retain each symmetry are reduced to conditions to the elemental operators as summarized in Table I. This simplification is based on the fact that all of the operators $\tilde{G}, \tilde{S}(k)$, and $\tilde{\Phi}$ are described by exponentials of σ_3, and then they are commutative. However, when the parameters depend on position, the shift operator S is not commutative with gain-loss operator G_i and phase operator Φ_i. Thus, we need to consider conditions for operators $SG_i\Phi_i$ as a whole. For example, the condition to retain $\mathcal{PT}$ symmetry for the time-evolution operator is derived as follows. By substituting Eq. (35) into Eq. (34a), the left and right hand sides become

$$\text{LHS} = [(\mathcal{PT})\,C(\theta_1/2)\,(\mathcal{PT})^{-1}]\,[(\mathcal{PT})\,SG_2\Phi_2\,(\mathcal{PT})^{-1}]\cdots,$$

$$\text{RHS} = [C^{-1}(\theta_1/2)]\,[(SG_1\Phi_1)^{-1}]\cdots,$$

respectively. By comparing these two equations, we obtain the conditions to retain $\mathcal{PT}$ symmetry for the time-evolution operator of the nonunitary quantum walk in inhomogeneous systems as

$$(\mathcal{PT})C(\theta_i)(\mathcal{PT})^{-1} = C^{-1}(\theta_i), \tag{36a}$$

$$(\mathcal{PT})(SG_i\Phi_i)(\mathcal{PT})^{-1} = (SG_j\Phi_j)^{-1}, \tag{36b}$$

where $i, j = 1,2$ and $i \neq j$. From Eq. (36), we obtain conditions imposed on each position-dependent parameter to retain

$\mathcal{PT}$ symmetry as

$$\theta_i(n) = \theta_i(-n+q), \tag{37a}$$
$$g_{1,L}(n) = [g_{2,L}(-n+q+1)]^{-1}, \tag{37b}$$
$$g_{1,R}(n) = [g_{2,R}(-n+q-1)]^{-1}, \tag{37c}$$
$$\phi_{1,L}(n) = \phi_{2,L}(-n+q+1), \tag{37d}$$
$$\phi_{1,R}(n) = \phi_{2,R}(-n+q-1). \tag{37e}$$

We find that, on one hand, the parameter $\theta_i(n)$ of the coin operator is uncorrelated in time direction, which means that $\theta_1(n)$ and $\theta_2(n)$ can be determined independently. On the other hand, parameters of gain-loss and phase operators have strict restrictions in time direction as well as in position space. We note that when conditions in Eqs. (37b) and (37c) are satisfied, the absolute value of the determinant of the time-evolution operator U in inhomogeneous systems remains to be one, even though the determinant of each G_i is not one. We should also recall that while the conditions Eq. (37) guarantee that the time-evolution operator has $\mathcal{PT}$ symmetry, they do not guarantee that eigenvectors of the time-evolution operator are those of the $\mathcal{PT}$-symmetry operator.

In the same way, we can obtain conditions to preserve PCS and PHS for the time-evolution operator in inhomogeneous systems. We find that PCS is maintained under the following conditions:

$$\theta_i(n) = \theta_i(-n+q), \tag{38a}$$
$$g_{1,L}(n) = [g_{2,L}(-n+q+1)]^{-1}, \tag{38b}$$
$$g_{1,R}(n) = [g_{2,R}(-n+q-1)]^{-1}, \tag{38c}$$
$$\phi_{1,L}(n) = -\phi_{2,L}(-n+q+1), \tag{38d}$$
$$\phi_{1,R}(n) = -\phi_{2,R}(-n+q-1). \tag{38e}$$

Comparing the above conditions, Eq. (38), with those for $\mathcal{PT}$ symmetry in Eq. (37), we understand that while Eqs. (38a)–(38c) are the same as Eqs. (37a)–(37c), the conditions on phases $\phi_{i,\sigma}(n)$ to retain $\mathcal{PT}$ symmetry and PCS cannot be simultaneously satisfied unless $\phi_{i,\sigma}(n) = 0$. This gives another conclusion that PHS is retained only if $\phi_{i,\sigma}(n) = 0$ since PHS can be defined as the combination of $\mathcal{PT}$ symmetry and PCS, $\Xi = (\mathcal{PT})(\mathcal{P}\Gamma)$. By combining Eqs. (37) and (38), we also understand that there is no constraint on $\theta_i(n)$ and $g_{i,\sigma}(n)$ to retain PHS.

IV. APPLICATIONS

Finally, we apply results to retain various symmetries obtained in Sec. III into specific models of nonunitary quantum walks. At first, we identify symmetries of the nonunitary quantum walk realized in the experiment [45]. Second, we show the numerical results of the walker's time evolution in the homogeneous system considered in Sec. III A. For the other example, we demonstrate that, for an inhomogeneous nonunitary quantum walk where four distinct spatial regions exist, the time-evolution operator possesses $\mathcal{PT}$ symmetry and the quasienergy becomes entirely real.

A. Symmetries satisfied in the experiment

Here, we directly identify symmetries of the nonunitary quantum walk realized in the experiment [45] from the time-evolution operator. The time-evolution operator in the experiment, U_{ex}, is given by Eq. (3) by assigning the following parameters:

$$\theta_1(n) = \theta_2(n) = \pi/4, \tag{39a}$$
$$g_{1,L}(n) = [g_{2,L}(n)]^{-1} = e^{+\gamma_0}, \tag{39b}$$
$$g_{1,R}(n) = [g_{2,R}(n)]^{-1} = e^{-\gamma_0}, \tag{39c}$$
$$\phi_{1,L}(n) = \phi_{2,L}(n) = 0, \tag{39d}$$
$$\phi_{1,R}(n) = \phi_{2,R}(n) = \begin{cases} -\phi_0 & \text{for mod}(n+3,4) = 1, 2, \\ +\phi_0 & \text{for mod}(n+3,4) = 3, 0. \end{cases} \tag{39e}$$

The quasienergy of this time-evolution operator becomes

$$\cos(\pm\varepsilon) = -\tfrac{1}{2}\cos\phi_0\cosh(2\gamma_0) \pm \sqrt{f_k(\gamma_0,\phi_0)}, \tag{40}$$

where

$$f_k(\gamma_0,\phi_0) = \tfrac{1}{8}[\cosh(4\gamma_0)(\cos^2\phi_0 - 1) - 3\cos^2\phi_0 + 4 + \cos k].$$

Regarding $\mathcal{PT}$ symmetry, we can confirm that all parameters in Eq. (39) satisfy conditions in Eq. (37) to retain $\mathcal{PT}$ symmetry, especially, by choosing $q = -1$ for $\phi_{i,L}(n)$ which only depends on the position. Therefore, we can identify $\mathcal{PT}$ symmetry of the nonunitary time-evolution operator U_{ex} with the symmetry operator in Eq. (33a).

From Eq. (40) and Fig. 5, we expect that the time-evolution operator U_{ex} also has PHS and PCS because there appear pairs with the opposite quasienergies $\pm\varepsilon$. However, as shown in Sec. III B, the finite $\phi_{i,\sigma}(n)$ prevents PHS and PCS. This problem is solved by introducing a modified PHS operator with a position shift by r as

$$\Xi_r = \sum_n |n+r\rangle\langle n| \otimes \sigma_3\mathcal{K}. \tag{41}$$

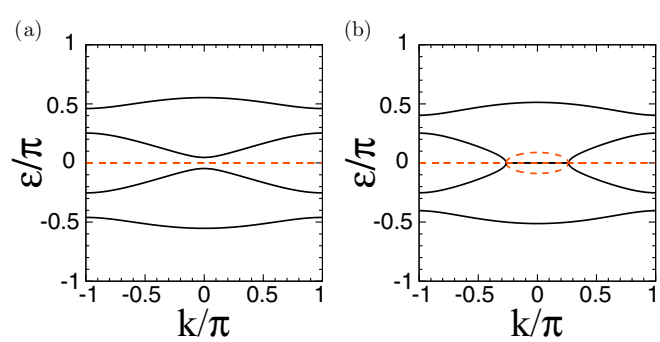

FIG. 5. The quasienergy as a function of k in Eq. (40) with various gain-loss parameters when $\phi_0 = 6\pi/5$. The solid (dashed) curve represents the real (imaginary) part of the quasienergy. (a) When $e^{\gamma} = 1.1$, the quasienergy is entirely real. (b) When $e^{\gamma} = 1.4$, a part of the quasienergy becomes complex. In both cases, quasienergy exists being symmetric with respect to $\varepsilon = 0$.

By using the modified PHS operator Ξ_r, the condition on the phase parameter to satisfy $\Xi_r U \Xi_r^{-1} = U$ is derived as

$$\phi_{i,\sigma}(n) = -\phi_{i,\sigma}(n+r). \tag{42}$$

Inputting $r = 2$, we confirm that the phase parameter in Eq. (39e) satisfies Eq. (42). Therefore, the time-evolution operator $U_{\rm ex}$ also preserves modified PHS.

B. Time evolution of probability distributions of homogeneous nonunitary quantum walks

Next, we numerically demonstrate the time evolution of probability distributions of nonunitary quantum walks in homogeneous systems. To this end, we employ the time-evolution operator in Eq. (14). We note that we define the probability distribution at a position n at a time t as

$$|\psi_n(t)|^2 = |\psi_{n,L}(t)|^2 + |\psi_{n,R}(t)|^2$$

even for nonunitary quantum walks although, in non-Hermitian quantum mechanics, the biorthogonality of eigenvectors (of a Hamiltonian or time-evolution operator) should be taken into account for normalized inner products. Because of this, the sum of the probability distributions over the position space

$$P(t) = \sum_n |\psi_n(t)|^2$$

need not be one for the nonunitary quantum walk, while $P(t) = 1$ for the unitary quantum walk. This choice stems from the fact that the quantity $|\psi_n(t)|^2$ calculated numerically agrees well with the intensity distribution of laser pulses observed experimentally in the optical-fiber loops with loss as reported in Ref. [38].

In Fig. 6, we show numerical results on the time evolution for the homogeneous quantum walk in Eq. (14). The parameters are the same with the parameter set in Fig. 3, namely, (a) $e^{\gamma} = 1$ (the unitary quantum walk), (b) $e^{\gamma} = 1.1$ (the nonunitary quantum walk with entirely real quasienergy), (c) $e^{\gamma} = 1.34\ldots$ (the nonunitary quantum walk at the exceptional point), and (d) $e^{\gamma} = 1.5$ (the nonunitary quantum walk with complex quasienergy). Comparing the probability distributions in Figs. 6(a) and 6(b), when

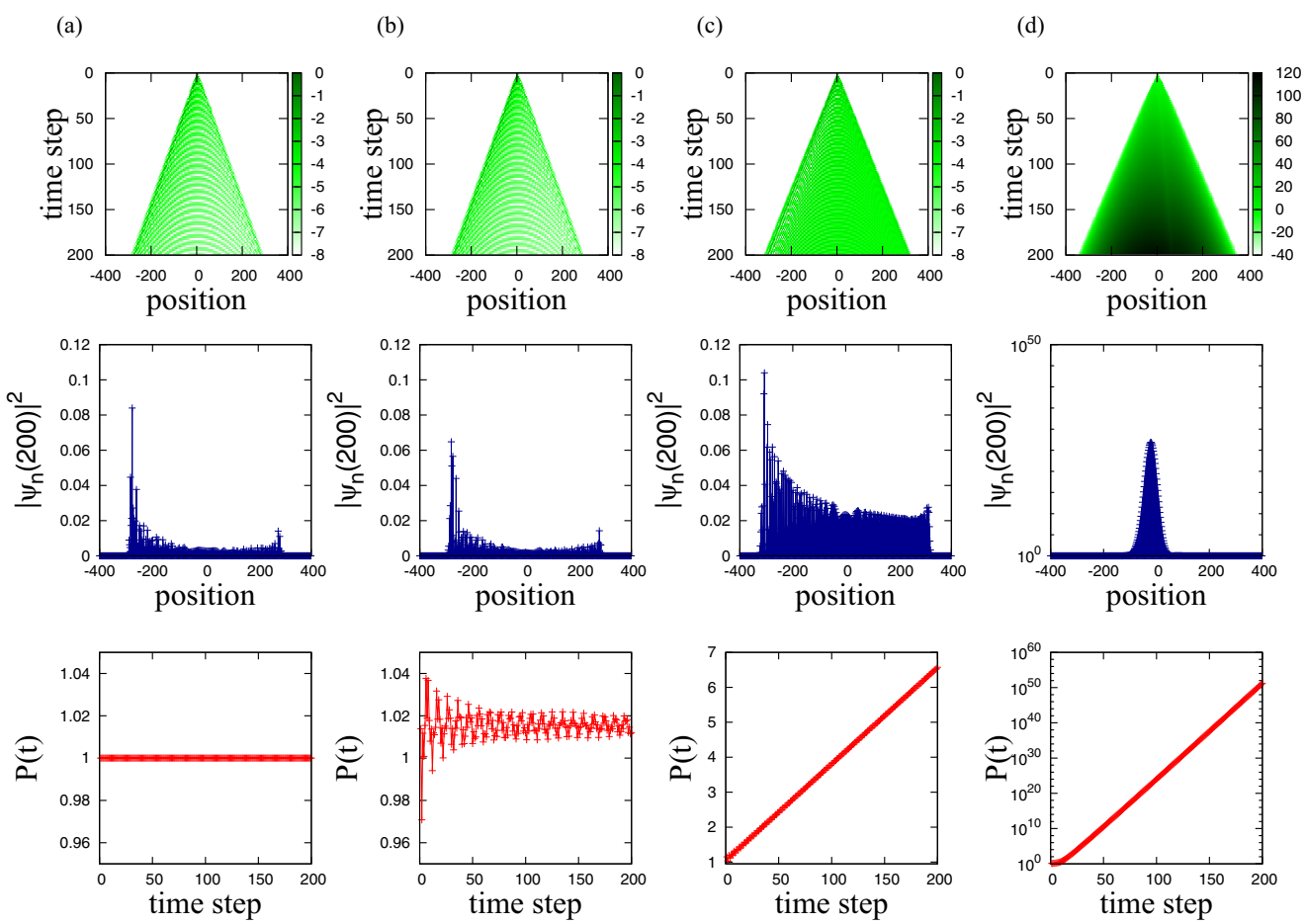

FIG. 6. The time evolution for the quantum walk in the homogeneous system with various gain-loss parameters: (a) $e^{\gamma} = 1$ (the unitary quantum walk), (b) $e^{\gamma} = 1.1$ (the nonunitary quantum walk with entirely real quasienergy), (c) $e^{\gamma} = 1.34\ldots$ (the nonunitary quantum walk at the exceptional point), and (d) $e^{\gamma} = 1.5$ (the nonunitary quantum walk with complex quasienergy). The other parameters $\theta_1 = \pi/4, \theta_2 = -\pi/7, \phi = 0$, and the initial state $|\psi(0)\rangle = |0\rangle \otimes |R\rangle$ are used for all cases (a)–(d). Top panels: The contour maps of the logarithm of the probability distribution $\ln[|\psi_n(t)|^2]$ in the position and time plane. Middle panels: The probability distributions after 200 time steps $|\psi_n(t = 200)|^2$. Bottom panels: The time step dependence of the sum of the probability distributions $P(t)$.

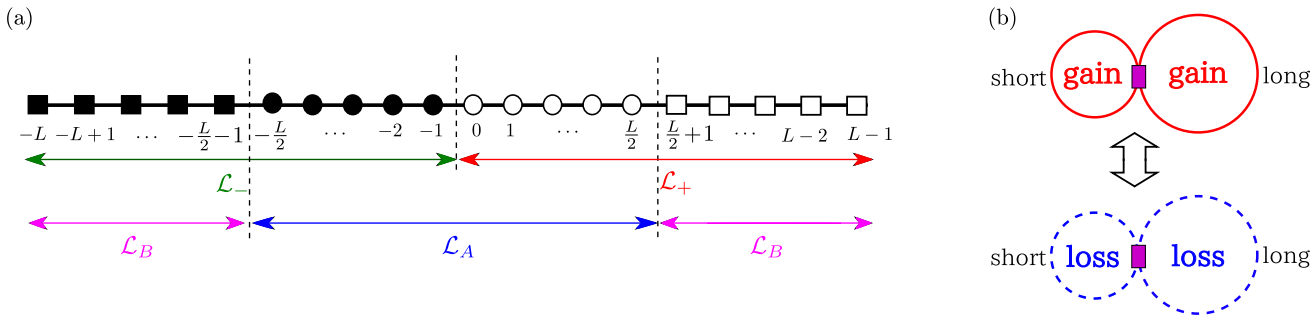

FIG. 7. (a) A schematic view of the nonunitary quantum walk with four distinct spatial regions. (b) A schematic view to explain gain-loss operations in the experiment by the optical-fiber loops.

the nonunitary quantum walk has entirely real quasienergy, the time evolution is not largely different from that of the unitary quantum walk. One exception is that the sum of the probability distribution $P(t)$ exhibits tiny oscillations around $P(t) \approx 1$ with time in the nonunitary case [Fig. 6(b), bottom], while $P(t) = 1$ in the unitary quantum walk [Fig. 6(a), bottom].

However, as increasing γ further, the time evolution of the nonunitary quantum walk drastically changes. At the exceptional point, the sum of the probability distribution $P(t)$ grows linearly with time as shown in Fig. 6(c), bottom, and when part of the quasienergies become complex, $P(t)$ grows exponentially with time as shown in Fig. 6(d), bottom. Remarkably, in the latter case, the probability distribution after 200 time steps is well approximated by the Gaussian distribution [Fig. 6(d), middle], in contrast with other cases (a)–(c). We note that linear and exponential growths of the sum of the probability distributions $P(t)$ are observed in Ref. [45] under a different setup, and the Gaussian distribution of the probability distribution is also reported in Refs. [24,38]. Therefore, these observations which are available by experiments can be considered as a manifestation of nonunitary time evolution.

C. Nonunitary quantum walks with four distinct regions

Although we can construct various time-evolution operators of nonunitary quantum walks in inhomogeneous systems with $\mathcal{PT}$ symmetry by employing the conditions in Eq. (37), keeping a real number of the quasienergy requires the additional condition that eigenstates of the time-evolution operator are those of the $\mathcal{PT}$-symmetry operator. Since it is our empirical fact that the additional condition is often broken in systems with strongly position-dependent parameters, here we treat a rather moderate inhomogeneous nonunitary quantum walk as shown in Fig. 7(a). This system has four distinct spatial regions with different parameters by combinations of $\mathcal{L}_{A/B}$ and $\mathcal{L}_{+/-}$ where the regions are defined as

$$\begin{aligned}
\mathcal{L}_A &: \quad -L/2 \leqslant n \leqslant L/2,\\
\mathcal{L}_B &: \quad n \leqslant -L/2-1, \quad n \geqslant L/2+1,\\
\mathcal{L}_+ &: \quad n \geqslant 0,\\
\mathcal{L}_- &: \quad n \leqslant -1.
\end{aligned}$$

Taking account of Eq. (37) with $q = 0$, we choose parameters of the elemental operators as follows:

$$\theta_1(n) = \begin{cases} +\pi/4 & n \in \mathcal{L}_A, \\ -\pi/8 & n \in \mathcal{L}_B, \end{cases} \tag{43a}$$

$$\theta_2(n) = \begin{cases} -\pi/3 & n \in \mathcal{L}_A, \\ +\pi/6 & n \in \mathcal{L}_B, \end{cases} \tag{43b}$$

$$g_{1,L}(n) = [g_{2,L}(-n+1)]^{-1} = \begin{cases} 1.1 & n \in \mathcal{L}_-, \\ 1.2 & n \in \mathcal{L}_+, \end{cases} \tag{43c}$$

$$g_{1,R}(n) = [g_{2,R}(-n+1)]^{-1} = \begin{cases} 1.2 & n \in \mathcal{L}_-, \\ 1.1 & n \in \mathcal{L}_+, \end{cases} \tag{43d}$$

$$\phi_{1,L}(n) = \phi_{2,L}(-n+1) = \begin{cases} \pi/4 & n \in \mathcal{L}_-, \\ \pi/8 & n \in \mathcal{L}_+, \end{cases} \tag{43e}$$

$$\phi_{1,R}(n) = \phi_{2,R}(-n+1) = \begin{cases} -\pi/3 & n \in \mathcal{L}_-, \\ -\pi/6 & n \in \mathcal{L}_+. \end{cases} \tag{43f}$$

We emphasize that $\theta_i(n)$ is symmetric with respect to the origin of position space, while $g_{i,\sigma}(n)$ and $\phi_{i,\sigma}(n)$ are not. We also remark that the first (second) gain-loss operator $G_{1(2)}$ only amplifies (dumps) wave function amplitudes of both left and right mover components as shown in Fig. 7(b), in contrast to the experimental setup in Fig. 1(a).

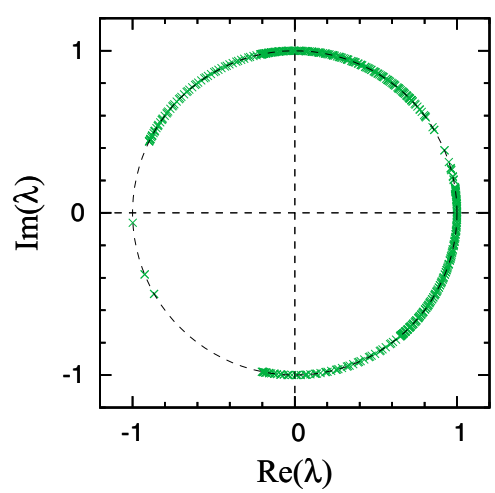

FIG. 8. The eigenvalue λ (green crossed) of the time-evolution operator of the nonunitary quantum walk with parameters in Eq. (43) plotted on a complex plain.

We numerically calculate eigenvalues of the time-evolution operator U assigned the above parameters by imposing periodic boundary conditions to both ends $L-1$ and $-L$ with $L=128$. As shown in Fig. 8 we clearly see that all eigenvalues stay on a unit circle in a complex plane, which indicates that the quasienergy is entirely real. Furthermore, eigenvalues are not symmetric with respect to $\varepsilon = 0,\pi$, because the position-dependent phase parameters $\phi_{i,\sigma}(n)$ break both PHS and PCS.

V. SUMMARY AND DISCUSSION

We have explicitly defined the $\mathcal{PT}$-symmetry operator for the time-evolution operator of the nonunitary quantum walk given in Eq. (3), and identified necessary and sufficient conditions, Eq. (37), on position-dependent parameters of the elemental operators to retain $\mathcal{PT}$ symmetry. Taking account of the conditions, we have succeeded in clarifying the presence of $\mathcal{PT}$ symmetry of the nonunitary quantum walk realized in the experiment by using optical-fiber loops [45] from the time-evolution operator. This has been accomplished for the first time by employing the concept of the symmetry time frame which had been developed in the recent work on topological phases of quantum walks [44]. At the same time, we have also studied extra symmetries embedded in the time-evolution operator of the nonunitary quantum walk, such as chiral symmetry, PHS, PCS, and so on. In Sec. IV B, we have numerically demonstrated the time evolution of probability distributions for the homogeneous nonunitary quantum walk, and shown that those of the nonunitary quantum walk with entirely real quasienergy are completely different from those with complex quasienergy. Besides, we have also demonstrated in Sec. IV C that the inhomogeneous nonunitary quantum walk which has $\mathcal{PT}$ symmetry and even possesses entirely real quasienergy is possible.

We believe that the result obtained in the present work stimulates further developments on $\mathcal{PT}$ symmetry of nonunitary time-evolution operators which has not yet been studied enough, compared with non-Hermitian Hamiltonians. Also, the conditions Eq. (37) would strongly support the experiment by using the optical-fiber loops [45] as the versatile platform for studying phenomena originating in $\mathcal{PT}$ symmetry. Besides this, although we have focused on the optical-fiber setup in the present work, our result can be straightforwardly applied to other setups of the quantum walk. Furthermore, we can easily generalize our theory to the nonunitary quantum walk only with dissipation, which would be much easier to realize in various experimental setups. In addition, since we have shown that the nonunitary quantum walk can retain important symmetries to establish topological phases, it would be interesting to study topological phases and corresponding edge states of the nonunitary quantum walk, which we will report on elsewhere.

An important open problem is to identify a generalized condition to retain real quasienergy of the nonunitary quantum walk. According to progress on $\mathcal{PT}$ symmetry of non-Hermitian Hamiltonians, it is already known that the argument on $\mathcal{PT}$ symmetry can be generalized as follows: if a Hamiltonian H satisfies a pseudo-Hermiticity condition $\eta H \eta^{-1} = H^{\dagger}$ with a positive operator η which may not be related to parity symmetry, eigenenergy could become real [54,55]. Indeed, we observed possibly related phenomena in our nonunitary quantum walk setup because quasienergy becomes entirely real even when $\theta_1(n)$ is completely random in position space. This suggests the possibility of retaining real quasienergy of the nonunitary time-evolution operator without strong constraint on the position space. We leave this issue as a future work.

ACKNOWLEDGMENTS

We thank Y. Asano, Y. Matsuzawa, A. Suzuki, and K. Yakubo for helpful discussions. This work was supported by a Grant-in-Aid for Scientific Research on Innovative Areas "Topological Materials Science" (JSPS KAKENHI Grant No. 16H00975) and also JSPS KAKENHI (Grants No. 16K17760 and No. 16K05466).

[1] N. Moiseyev, *Non-Hermitian Quantum Mechanics* (Cambridge University Press, Cambridge, 2011).

[2] N. Hatano and D. R. Nelson, Vortex pinning and non-Hermitian quantum mechanics, Phys. Rev. B **56**, 8651 (1997); Non-Hermitian delocalization and eigenfunctions, *ibid.* **58**, 8384 (1998).

[3] T. Gao, E. Estrecho, K. Y. Bliokh, T. C. H. Liew, M. D. Fraser, S. Brodbeck, M. Kamp, C. Schneider, S. Ho, Y. Yamamoto, F. Nori, Y. S. Kivshar, A. G. Truscott, R. G. Dall, and E. A. Ostrovskaya, Observation of non-Hermitian degeneracies in a chaotic exciton-polariton billiard, Nature (London) **526**, 554 (2015).

[4] C. M. Bender and S. Boettcher, Real Spectra in non-Hermitian Hamiltonians Having $\mathcal{PT}$ Symmetry, Phys. Rev. Lett. **80**, 5243 (1998).

[5] C. M. Bender, S. Boettcher, and P. N. Meisinger, $\mathcal{PT}$-symmetric quantum mechanics, J. Math. Phys. **40**, 2201 (1999).

[6] C. M. Bender, Making sense of non-Hermitian Hamiltonians, Rep. Prog. Phys. **70**, 947 (2007).

[7] D. C. Brody, Biorthogonal quantum mechanics, J. Phys. A **47**, 3 (2014).

[8] M. A. Miri, P. LiKamWa, and D. N. Christodoulides, Large-area single-mode parity-time-symmetric laser amplifiers, Opt. Lett. **37**, 764 (2012).

[9] H. Schomerus, Topologically protected midgap states in complex photonic lattices, Opt. Lett. **38**, 1912 (2013).

[10] C. Poli, M. Bellec, U. Kuhl, F. Mortessagne, and H. Schomerus, Selective enhancement of topologically induced interface states in a dielectric resonator chain, Nat. Commun. **6**, 6710 (2015).

[11] Z. Lin, H. Ramezani, T. Eichelkraut, T. Kottos, H. Cao, and D. N. Christodoulides, Unidirectional Invisibility Induced by $\mathcal{PT}$-Symmetric Periodic Structures, Phys. Rev. Lett. **106**, 213901 (2011).

[12] A. Mostafazadeh, Invisibility and $\mathcal{PT}$ symmetry, Phys. Rev. A **87**, 012103 (2013).

[13] Y. C. Hu and T. L. Hughes, Absence of topological insulator phases in non-Hermitian $\mathcal{PT}$-symmetric Hamiltonians, Phys. Rev. B **84**, 153101 (2011).

[14] K. Esaki, M. Sato, K. Hasebe, and M. Kohmoto, Edge states and topological phases in non-Hermitian systems, Phys. Rev. B **84**, 205128 (2011).

[15] S. Longhi, Bloch Oscillations in Complex Crystals with $\mathcal{PT}$ Symmetry, Phys. Rev. Lett. **103**, 123601 (2009).

[16] C. M. Bender, D. C. Brody, and H. F. Jones, Complex Extension of Quantum Mechanics, Phys. Rev. Lett. **89**, 270401 (2002).

[17] S. Garmon, M. Gianfreda, and N. Hatano, Bound states, scattering states, and resonant states in $\mathcal{PT}$-symmetric open quantum systems, Phys. Rev. A **92**, 022125 (2015).

[18] P. G. Kevrekidis, J. Cuevas-Maraver, A. Saxena, F. Cooper, and A. Khare, Interplay between parity-time symmetry, supersymmetry, and nonlinearity: An analytically tractable case example, Phys. Rev. E **92**, 042901 (2015).

[19] C. M. Bender, M. Gianfreda, and S. P. Klevansky, Systems of coupled $\mathcal{PT}$-symmetric oscillators, Phys. Rev. A **90**, 022114 (2014).

[20] N. M. Chtchelkatchev, A. A. Golubov, T. I. Baturina, and V. M. Vinokur, Stimulation of the Fluctuation Superconductivity by $\mathcal{PT}$ Symmetry, Phys. Rev. Lett. **109**, 150405 (2012).

[21] M. C. Zheng, D. N. Christodoulides, R. Fleischmann, and T. Kottos, $\mathcal{PT}$ optical lattices and universality in beam dynamics, Phys. Rev. A **82**, 010103 (2010).

[22] S. Kalish, Z. Lin, and T. Kottos, Light transport in random media with $\mathcal{PT}$ symmetry, Phys. Rev. A **85**, 055802 (2012).

[23] O. Bendix, R. Fleischmann, T. Kottos, and B. Shapiro, Exponentially Fragile $\mathcal{PT}$ Symmetry in Lattices with Localized Eigenmodes, Phys. Rev. Lett. **103**, 030402 (2009).

[24] S. Longhi, Spectral singularities and Bragg scattering in complex crystals, Phys. Rev. A **81**, 022102 (2010).

[25] A. Guo and G. J. Salamo, Observation of $\mathcal{PT}$-Symmetry Breaking in Complex Optical Potentials, Phys. Rev. Lett. **103**, 093902 (2009).

[26] C. E. Rüter, K. G. Kakris, R. El-Ganainy, D. N. Christodoulides, M. Mordechai, and D. Kip, Observation of parity-time symmetry in optics, Nat. Phys. **6**, 192 (2010).

[27] B. Peng, S. K. Özdemir, F. Lei, F. Monifi, M. Gianfreda, G. L. Long, S. Fan, F. Nori, C. M. Bender, and L. Yang, Parity-time-symmetric whispering-gallery microcavities, Nat. Phys. **10**, 394 (2014).

[28] B. Peng, S. K. Özdemir, S. Rotter, H. Yilmaz, M. Liertzer, F. Monifi, C. Bender, F. Nori, and L. Yang, Loss-induced suppression and revival of lasing, Science **346**, 328 (2014).

[29] L. Feng, Z. J. Wong, R-M. Ma, Y. Wang, and X. Zhang, Single-mode laser by parity-time-symmetry breaking, Science **346**, 972 (2014).

[30] H. Hodaei, M-A. Miri, M. Heinrich, D. N. Christodoulides, and M. Khajavikhan, Parity-time-symmetric microring lasers, Science **346**, 975 (2014).

[31] J. Kempe, Quantum random walks: An introductory overview, Contemp. Phys. **44**, 307 (2003).

[32] A. Ambainis, Quantum walks and their algorithmic applications, Int. J. Quantum Inform. **01**, 507 (2003).

[33] M. Karski, L. Förster, J.-M. Choi, A. Steffen, W. Alt, D. Meschede, and A. Widera, Quantum walk in position space with single optically trapped atoms, Science **325**, 174 (2009).

[34] H. Schmitz, R. Matjeschk, Ch. Schneider, J. Gluekert, M. Enderlein, T. Huber, and T. Schaetz, Quantum Walk of a Trapped Ion in Phase Space, Phys. Rev. Lett. **103**, 090504 (2009).

[35] F. Zähringer, G. Kirchmair, R. Gerritsma, E. Solano, R. Blatt, and C. F. Roos, Realization of a Quantum Walk with One and Two Trapped Ions, Phys. Rev. Lett. **104**, 100503 (2010).

[36] A. Schreiber, K. N. Cassemiro, V. Potoček, A. Gábris, P. J. Mosley, E. Andersson, I. Jex, and Ch. Silberhorn, Photons Walking the Line: A Quantum Walk with Adjustable Coin Operations, Phys. Rev. Lett. **104**, 050502 (2010).

[37] M. A. Broome, A. Fedrizzi, B. P. Lanyon, I. Kassal, A. Aspuru-Guzik, and A. G. White, Discrete Single-Photon Quantum Walks with Tunable Decoherence, Phys. Rev. Lett. **104**, 153602 (2010).

[38] A. Regensburger, C. Bersch, B. Hinrichs, G. Onishchukov, A. Schreiber, C. Silberhorn, and U. Peschel, Photon Propagation in a Discrete Fiber Network: An Interplay of Coherence and Losses, Phys. Rev. Lett. **107**, 233902 (2011).

[39] A. Schreiber, A. Gábris, P. R. Rohde, K. Laiho, M. Štefaňák, V. Potoček, C. Hamilton, I. Jex, and Ch. Sil-berhorn, A 2D quantum walk simulation of two-particle dynamics, Science **336**, 55 (2012).

[40] P. Xue, H. Qin, and B. Tang, Trapping photons on the line: Controllable dynamics of a quantum walk, Sci. Rep. **4**, 4825 (2014).

[41] A. Schreiber, K. N. Cassemiro, V. Potoček, A. Gaábris, I. Jex, and Ch. Silberhorn, Decoherence and Disorder in Quantum Walks: From Ballistic Spread to Localization, Phys. Rev. Lett. **106**, 180403 (2011).

[42] A. Crespi, R. Osellame, R. Ramponi, V. Giovannetti, R. Fazio, L. Sansoni, F. D. Nicola, F. Sciarrino, and P. Mataloni, Anderson localization of entangled photons in an integrated quantum walk, Nat. Photonics **7**, 322 (2013).

[43] M. Wimmer, A. Regensburger, C. Bersch, M-A. Miri, S. Batz, G. Onishchukov, D. N. Christodoulides, and U. Peschel, Optical diametric drive acceleration through action-reaction symmetry breaking, Nat. Phys. **9**, 780 (2011).

[44] T. Kitagawa, M. A. Broome, A. Fedrizzi, M. S. Rudner, E. Berg, I. Kassal, A. Aspuru-Guzik, E. Demler, and A. G. White, Observation of topologically protected bound states in photonic quantum walks, Nat. Commun. **3**, 882 (2012).

[45] A. Regensburger, C. Bersch, M-A. Miri, G. Onishchukov, D. N. Christodoulides, and U. Peschel, Parity-time synthetic photonic lattices, Nature (London) **488**, 167 (2012).

[46] A. Regensburger, M.-A. Miri, C. Bersch, J. Nager, G. Onishchukov, D. N. Christodoulides, and U. Peschel, Observation of Defect States in $\mathcal{PT}$-Symmetric Optical Lattices, Phys. Rev. Lett. **110**, 223902 (2013).

[47] M. Wimmer, A. Regensburger, M.-A. Miri, C. Bersch, D. N. Christodoulides, and U. Peschel, Observation of optical solitons in $\mathcal{PT}$-symmetric lattices, Nat. Commun. **6**, 7782 (2015).

[48] J. K. Asbóth and H. Obuse, Bulk-boundary correspondence for chiral symmetric quantum walks, Phys. Rev. B **88**, 121406(R) (2013).

[49] T. Kitagawa, M. S. Rudner, E. Berg, and E. Demler, Exploring topological phases with quantum walks, Phys. Rev. A **82**, 033429 (2010).

[50] H. Obuse and N. Kawakami, Topological phases and delocalization of quantum walks in random environments, Phys. Rev. B **84**, 195139 (2011).

[51] J. K. Asbóth, Symmetries, topological phases, and bound states in the one-dimensional quantum walk, Phys. Rev. B **86**, 195414 (2012).

[52] H. Obuse, J. K. Asbóth, Y. Nishimura, and N. Kawakami, Unveiling hidden topological phases of a one-dimensional Hadamard quantum walk, Phys. Rev. B **92**, 045424 (2015).

[53] C. M. Bender, M. V. Berry, and A. Mandilara, Generalized $\mathcal{PT}$ symmetry and real spectra, J. Phys. A: Math. Gen. **35**, L467 (2002).

[54] A. Mostafazadeh, Pseudo-Hermiticity versus $\mathcal{PT}$ symmetry: The necessary condition for the reality of the spectrum of a non-Hermitian Hamiltonian, J. Math. Phys. **43**, 205 (2002); Pseudo-Hermiticity versus $\mathcal{PT}$ symmetry II: A complete characterization of non-Hermitian Hamiltonians with a real spectrum, *ibid.* **43**, 2814 (2002); Pseudo-Hermiticity versus $\mathcal{PT}$ symmetry III: Equivalence of pseudo-Hermiticity and the presence of antilinear symmetries, *ibid.* **43**, 3944 (2002).

[55] A. Mostafazadeh, Pseudo-unitary operators and pseudo-unitary quantum dynamics, J. Math. Phys. **45**, 932 (2004).